Annotation sheet

Name: Hector

Surname: Calvopina

Title in Czech: CFD simulace přenosu tepla v míchané nádobě s ponornou trubicí

Title in English: CFD simulation of heat transfer in an agitated vessel with a draft tube

Scope of work: number of pages: 52
number of figures: 13
number of tables: 5
number of appendices: 5

Academic year: 2017/2018

Language: English

Department: Process Engineering

Specialization: Process Engineering

Supervisor: Ing. Karel Petera, Ph. D.

Reviewer:

Submitter: Czech Technical University in Prague. Faculty of Mechanical Engineering, Department of Process Engineering

Annotation - Czech: Proveďte výzkum literatury týkající se přenosu tepla v rozrušených nádobách. Vytvořte model daného modelu v ANSYS CFD. Provést numerické simulace přenosu tepla v míchané nádobě pro různé otáčky a vyhodnotit koeficienty přenosu tepla v dolní a svislé stěně. Shrnout metodiku použitou v práci a navrhnout možné zlepšení postupu řešení.

Annotation – English: Make a literature research concerning the heat transfer in agitated vessels. Create a model of the given model in ANSYS CFD. Perform numerical simulations of heat transfer n the agitated vessel for different rotation speeds and evaluate heat transfer coefficients at the bottom and vertical wall. Summarize the methodology used in the thesis and propose possible improvements of the solution procedure.

Keywords: agitated vessel, heat transfer, sliding mesh, Nusselt number, CFD.

Utilization: For Department of Process Engineering, Czech Technical University in Prague.

Declaration

I hereby declare that I have completed this thesis entitled **CFD simulation of heat transfer in an agitated vessel with a draft tube** independently with consultations with my supervisor and I have attached a full list of used references and citations.

I do not have a compelling reason against the use of the thesis within the meaning of Section 60 of the Act No. 121/2000 Coll., on copyright, rights related to copyright and amending some taws (Copyright Act).

In Prague …………………. …..…………………….......

Name and Surname ,

ACKNOWLEDGEMENT

I would like to thank my thesis supervisor Ing. Karel Petera, PhD., the door of his office was always open whenever I run into a trouble or had any question about my work. I am gratefully indebted to his for his help on this thesis.

I would also like to express my very profound gratitude to my mom Gloria, my sister Karen and the love of my life, Tatiana. They provided me unfailing support and continuous encouragement throughout my years of study.

Finally, I would like to dedicate this thesis to my father, I know he would be proud of me.

ABSTRACT

A CFD simulation of heat transfer in an agitated vessel with a draft tube was performed in ANSYS Fluent using the Sliding Mesh approach and the SST k-ω turbulent model. A grid independence study based on the number of time steps was made in order to select an appropriate size of the time step. Mean values of the Nusselt number as well as local values along the radial coordinate of the heat transfer surface are presented. Results are compared with data from previous simulations. Correlations describing the mean Nusselt number at the bottom and wall were obtained and compared with literature.

Keywords: agitated vessel, heat transfer, sliding mesh, Nusselt number, CFD.

TABLE OF CONTENTS

LIST OF FIGURES

LIST OF TABLES

NOTATIONS

a	thermal diffusivity [m^2/]
c	general constant Eqs. (21), (22)…
Cp	specific heat capacity [J/kg K]
d	diameter of the draft tube [mm]
dm	diameter of the impeller [mm]
D	diameter of the tank [mm]
h	distance from the bottom of the tank to the draft tube [mm]
H	height of the tank [mm]
m	general constant, Reynolds number exponent
N	rotational speed of the speed [RPM]
Nu	Nusselt number
Pr	Prandtl number
Re	Reynolds number
Tf	final temperature
$\vec{u}$	instantaneous velocity [m/s]
$\bar{u}$	mean velocity [m/s]
u'	fluctuating velocity component [m/s]
α	heat transfer coefficient [W/m^2 K]
λ	thermal conductivity [W/m K]
μ	dynamic viscosity [Pa s]
ν	kinematic viscosity [m^2/s]
ρ	density [kg/m^3]
μ_t	turbulent viscosity [Pa s]
k	turbulent kinetic energy [m^2/s^2]
ε	dissipation rate of the turbulent kinetic energy [m^2/s^3]
ω	specific dissipation of the turbulent kinetic energy [1/s]

INTRODUCTION

Mixing vessels are present in many industrial applications where many operations are dependent on a good agitation or mixing of fluids. "Generally, agitation refers to the action of forcing a fluid to flow in a circular pattern by mechanical means inside a vessel. Mixing usually implies the presence of two different elements in the same or different phase, e.g. a fluid and a powdered solid or two fluids, which are blended together to obtain a homogeneous solution." [Christie John Geankoplis, Transport Processes and Separation Process Principles, 2003.].

There are several purposes for agitating fluids, some of them are blending of two miscible liquids, dissolving solids in liquids, good homogenization of liquid in a system and increasing the intensity of heat and mass transfer. "Heat transfer rates and hence time of cooling or heating of agitated liquid is influenced by many parameters like geometry, process parameters, an impeller type and its rotation speed (mixing intensity)" [K. Petera et al, Transient measurement of heat transfer coefficient in agitated vessel, 2008].

A draft tube is a cylindrical tube with an axial flow impeller placed inside it. "A stream of liquid generated by an axial-flow impeller in an agitated vessel impacts the vessel bottom similarly as the stream of fluid leaving a round jet and impinging a plane surface. Some similarities should exist here, the main difference lies in the tangential velocity component generated by the rotating impeller" [K. Petera et al, Heat Transfer at the Bottom of a Cylindrical Vessel, 2017]. The relation between tangential and axial velocity components is known as swirl number (S).

Generally, the design of agitated vessels is based on the parameters obtained by experimental results on the laboratory scale models. This approach is widely used but the only problems are the investment cost and the construction time. Nowadays, a powerful tool known as Computational Fluid Dynamics (CFD) let us perform a preliminary design without the experimental stage and gives us some parameters to analyze the possible outcomes of the project.

COMPUTATIONAL FLUID DYNAMICS

Computational Fluid Dynamics (CFD) is the science of predicting fluid flow, heat and mass transfer, chemical reactions, and related phenomena. To predict these phenomena, CFD solves equations for conservation of mass, momentum, energy etc. CFD can provide detailed information on the fluid flow behavior:

- Distribution of pressure, velocity, temperature, etc.
- Forces like Lift, Drag (external flows, Aero, Auto)
- Distribution of multiple phases (gas-liquid, gas-solid)
- Species composition (reactions, combustion, pollutants)
- Much more

CFD is used in all stages of the engineering process:

- Conceptual studies of new designs
- Detailed product development
- Optimization
- Troubleshooting
- Redesign

CFD analysis complements testing and experimentation by reducing total effort and cost required for experimentation and data acquisition.

A common CFD solver is based on the finite volume method. This means that the domain is discretized into a finite set of control volumes and general conservation (transport) equations for mass, momentum, energy, species, etc. are solved on this set of control volumes. Then partial differential equations are discretized into a system of algebraic equations and finally, all algebraic equations are then solved numerically to render the solution field [ANSYS Training material, 2014].

MAIN EQUATIONS

There are three main equations in CFD, they are based on the fundamental physical principles of conservation of mass (continuity equation), momentum (Navier Stokes equation) and energy (Fourier-Kirchhoff equation).

Continuity equation

The continuity equation represents the mass balance of a system (control volume). For incompressible fluids (fluids with constant density), it is described as:

$$\nabla \cdot \vec{u} = 0 \tag{1}$$

where vector $\vec{u}$ is velocity. For a Cartesian coordinate it can be expressed as:

$$\frac{\partial u_x}{\partial_x} + \frac{\partial u_y}{\partial_y} + \frac{\partial u_z}{\partial_z} = 0 \tag{2}$$

Navier-Stokes equation

The Navier-Stokes equation represents the momentum balance and is a special case of the Cauchy's equation. It's applied for uncompressible Newtonians fluids (constant density) and gravity forces instead of volume forces. This equation can be written as [Bird et al., 2007]:

$$\rho \left(\frac{\partial \vec{u}}{\partial t} + \vec{u} \cdot \nabla \vec{u} \right) = -\nabla p + \mu \nabla^2 \vec{u} + \rho \vec{g} \tag{3}$$

where vector $\vec{u}$ is velocity, ∇p is the gradient of pressure, μ is the dynamic viscosity, ρ is density and $\vec{g}$ is the gravity force.

Fourier-Kirchhoff equation

The Fourier-Kirchhoff equation is the basic equation describing heat transfer and for uncompressible fluids can be expressed as [Bird et al., 2007]:

$$\rho C_p \left(\frac{\partial T}{\partial t} + \vec{u} \cdot \nabla T \right) = \lambda \nabla^2 T + \vec{\vec{\tau}} : \vec{\vec{\Delta}} + \dot{Q}^{(g)} \tag{4}$$

Here the term $\vec{u} \cdot \nabla T$ is associated with the convective heat transfer, which vanishes when the velocity is zero. The first term on the right hand side of the equation represents the conductive heat transfer (when λ is constant and doesn't change with time or special

11

coordinate). The second term on the right hand side represents the double-dot product of the dynamic stress tensor ($\vec{\vec{\tau}}$) and the deformation rate tensor ($\vec{\vec{\Delta}}$) and $\dot{Q}^{(g)}$ represents the internal heat sources [K. Petera, Tutorial Momentum Heat and Mass Transfer 2017].

TURBULENCE MODELING

In the real world, most of the engineering flows are turbulent and turbulence is essentially a random process characterized by fluctuations of transported quantities such as flow velocity, pressure, temperature, etc. The instantaneous velocity of a real (turbulent) flow looks like this:
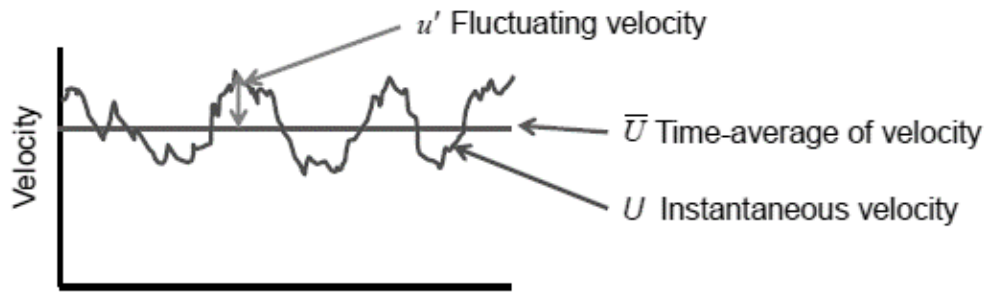
Figure 1 – Instant velocity in a turbulent flow [ANSYS Training material 2014].

Therefore, it can be described as:

$$\vec{u} = \bar{u} + u' \tag{5}$$

where $\bar{u}$ is the mean velocity and u' is the fluctuating velocity.

Because of the random behavior of a turbulent flow, it is not possible to perfectly describe the turbulence effects in a CFD simulation. But instead, a turbulence model is used.

Three basic approaches can be used to calculate turbulence flow:

Direct Numerical Simulation (DNS)
- It is technically possible to resolve every fluctuating motion in the flow.
- The grid must be very fine and time step very small.
- Demands increase with Reynolds number.
- This is only a research tool for lower Reynolds number flows
- Restricted to supercomputer applications.

Large Eddy Simulation (LES)
- 3D simulation is performed over many time steps.
- Only larger eddies are solved.
- Grid can be coarser and time steps larger than DNS.
- Less expensive than DNS but the computational demands are still too large for practical applications.

Reynolds Averaged Navier Stokes (RANS)
- Equations are solved for time averaged flow behavior.
- All turbulent motion is modeled.
- Many different models available.
- Main approach used by engineers.

By substituting Eq. (5) into the Navier –Stokes equation, we obtain the RANS equation for mean velocity:

$$\rho \left(\frac{\partial \bar{u}_i}{\partial t} + \bar{u}_k \frac{\partial \bar{u}_i}{\partial x_k} \right) = -\frac{\partial \bar{p}}{\partial x_i} + \frac{\partial}{\partial x_j} \left(\mu \frac{\partial \bar{u}_i}{\partial x_j} \right) + \frac{\partial R_{ij}}{\partial x_j} \tag{6}$$

where R_{ij} is the Reynolds stress tensor, which must be described by a turbulence model. The RANS models fall into one of two categories: Reynolds Stress Models (RSM), which derive a transport equation for the Reynolds Stress terms, but is a more complex model since there are more equations to solve and the Eddy Viscosity Models, which assume the stress is proportional to the strain (strain being the gradients of velocity. EVMs, based on the Boussineseq approximation of the turbulent (eddy) viscosity [Hinze, 1975], are the most widely used turbulence models for CFD with the Reynolds stress tensor is defined as follows:

$$R_{ij} = -\overline{\rho u_i' u_j'} = \mu_t \left(\frac{\partial \bar{u}_i}{\partial x_j} + \frac{\partial \bar{u}_j}{\partial x_i} \right) - \frac{2}{3} \mu_t \frac{\partial \bar{u}_k}{\partial x_k} \delta_{ij} - \frac{2}{3} \rho k \delta_{ij} \tag{7}$$

where μ_t the so called turbulent viscosity, which and defined as:

$$\mu_t = \rho \, C_\mu \frac{k^2}{\varepsilon} \tag{8}$$

where C_μ is an empirical constant, k is the turbulent kinetic energy and ε is the dissipation rate of the kinetic energy.

Some of the different models of the RANS-EVMs approach that we can find are: Spalart-Allmaras model, k - ε model, k - ω model, etc. The SST k-ω model (the one used in this project) offers similar benefits than the standard k-ω but is not overly sensitive to inlet boundary conditions and provides more accurate prediction of flow separation compared with other RANS models. In this model, ω is the specific dissipation rate and is defined as the relation between the kinetic energy (k) and the dissipation rate (ε):

$$\omega = \frac{\varepsilon}{k} \tag{9}$$

Thus, the turbulence viscosity for the SST k-ω model can be described as:

$$\mu_t = \rho \, C_\mu \frac{k}{\omega} \tag{10}$$

SST k-ω or Realizable k-ε are the recommended choice for standard cases [ANSYS Training material 2014].

TURBULENT BOUNDARY LAYER

A turbulent boundary layer consist of distinct regions, but for CFD, the most important are the viscous sublayer, immediately adjacent to the wall and the log-layer, slightly further away from the wall. Different turbulence models require different inputs depending on whether the simulation needs to resolve the viscous sublayer with mesh or not.

Near to the wall, the velocity changes rapidly. Using dimensionless velocity defined as:

$$u^+ = \frac{u}{u_t} \quad ; \quad u_t = \sqrt{\frac{\tau_{wall}}{\rho}} \tag{11}$$

where u is the velocity of the flow, τ_{wall} the wall shear stress and ρ the density of the fluid, and dimensionless distance from the wall defined as:

$$Y^+ = \frac{Y \, u_t}{u} \tag{12}$$

14

where Y is the distance from the wall, we can create a plot in logarithmic scale, which represents the dimensionless boundary layer profiles (Figure 2) and generally is the same for all flows:
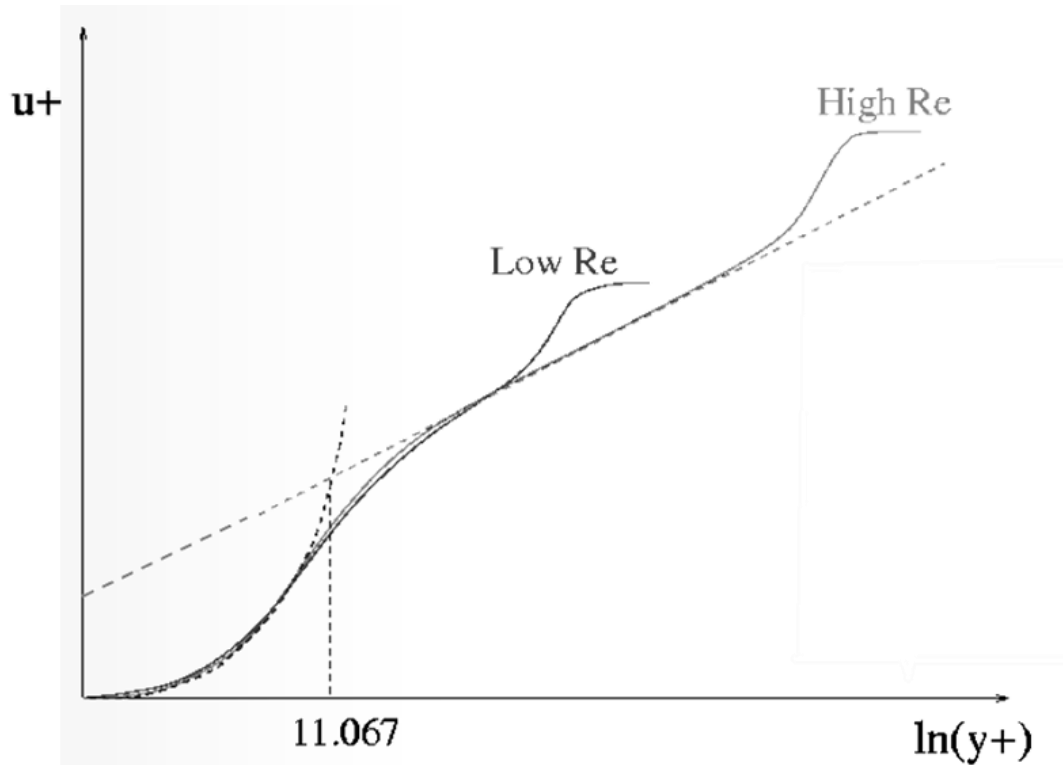
Figure 2 – Dimensionless boundary layer profile [ANSYS Training material 2014].

Near the wall, the velocity profile takes a predictable form, transitioning from linear in the viscous sublayer to logarithmic behavior in the log layer. As the Reynolds number increases, the logarithmic region extends to higher values of Y^+. This predictable boundary layer profile is valid for a wide range of flows.

In the near-wall region, the solution gradients are very high, but accurate calculations in this region are very important for the success of the simulation. There are two choices:

Wall functions

This approach uses the predictable dimensionless boundary layer shown on Figure 2, to calculate conditions at the wall (e.g. shear stress) when the centroid of the wall adjacent mesh is located in the log-layer. Commonly the value of Y^+ is between 30 and 300 and this approach should not be used if Y^+ is lower than 30.

In general, this approach is used when we are more interested in the mixing in the middle of the domain rather than the forces on the wall and can give us good results only in cases where the flow is aligned with the wall.

Viscous sublayer

With this approach, the whole viscous sublayer is described properly, the value of Y^+ should be close to 1. This ensures the mesh will be able to adequately resolve gradients in the sublayer.

This approach is used when the heat transfer on the wall in important for the simulation. Usually when this approach is used, the recommended turbulent model for most of the cases is SST $k - \omega$ [ANSYS Training material 2014].

GRID CONVERGENCE STUDY

The examination of the spatial convergence of a simulation is a method for determining the discretization error in a CFD simulation. The method involves performing the simulation on two or more finer grids, or two or more time steps. As the grid is refined (grid cells become smaller and the number of cells in the flow domain increase) or the time step is reduced, the spatial and temporal discretization errors, respectively, should asymptotically approaches zero, excluding computer round-off error, see Figure 3.
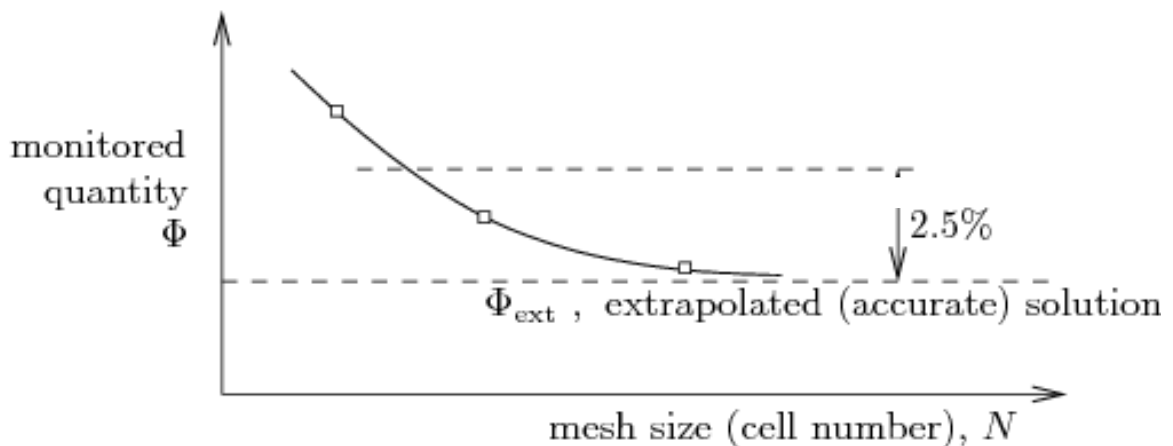
Figure 3 – Values of a monitored quantity according to the mesh size [K. Petera, Tutorial CFD, 2018].

To know the error band for the monitored quantities obtained from the finest grid solution is most often required. However, if many CFD simulations are performed for some analysis, a coarser grids should be used to decrease computational time. In this case, is necessary to determine the error on the coarser grid.

The dependency of the solution on the number of time steps can be described by the following equation:

$$\Phi = \Phi_{ext} + aN^p \tag{13}$$

where Φ represents the value of a the monitored quantity, N the number of time steps, Φext is the extrapolated value of the quantity for an infinitely large number of time steps and p the order of the solution accuracy (the lager the value, the better). The values of these parameters can be found from a solution of 3 equations for 3 different number of time steps.

$$\Phi_1 = \Phi_{ext} + aN_1^p$$

$$\Phi_2 = \Phi_{ext} + aN_2^p$$

$$\Phi_3 = \Phi_{ext} + aN_3^p$$

According to Celik [1993], the parameter p can be calculated as follows:

$$p = \frac{1}{ln\, r_{21}} \left| ln \left| \frac{\varepsilon_{32}}{\varepsilon_{21}} \right| + ln \left(\frac{r_{21}^p - s}{r_{32}^p - s} \right) \right| \tag{14}$$

where:

$$\varepsilon_{32} = \Phi_3 - \Phi_2, \qquad \varepsilon_{21} = \Phi_2 - \Phi_1$$

$$r_{21} = \frac{N_2}{N_1}, \qquad r_{32} = \frac{N_3}{N_2}$$

$$s = sign \frac{\varepsilon_{32}}{\varepsilon_{21}}$$

The absolute values and the sign function are used to take into account the case were the values of the monitored quantity are not decreasing or increasing monotonically, for example:

$$\Phi_1 < \Phi_2 , \Phi_2 > \Phi_3$$

To obtain the value of the parameter p, the Eq. 14 must solved with an iterative method. In Matlab for example, functions fzero can be used:

```
eps32 = Phi(3)-Phi(2);
eps21 = Phi(2)-Phi(1);
s = sign(eps32/eps21);

fq = @(p) log((r21.^p-s)./(r32.^p-s));
fp = @(p) p - 1/log(r21)*abs(log(abs(eps32/eps21)))+fq(p);
p = fzero(fp,1)
```

Then the extrapolated value of the monitored quantity can be expressed as:

$$\Phi_{ext} = \frac{\Phi_1\, r_{21}^p - \Phi_2}{r_{2q}^p - 1} \tag{15}$$

The accuracy of the solution for each value of Φ is expressed as the difference between the measured value and the extrapolated value and can be expressed in terms of the Grid Convergence Index (GCI). The smaller is the GCI the more accurate is the measured value. The GCI can be calculated as follows:

$$CGI_i = 1.25 \times \frac{|\Phi_{ext} - \Phi_i|}{\Phi_i} \times 100 \tag{16}$$

1.25 is the security factor. The CGI is expressed in percentage (%).

HEAT TRANSFER IN AGITATED VESSELS

The dimensionless numbers are used in order to analyze the heat transfer in agitated vessels. Dimensional analysis is a convenient tool, because reduces the number of dependent variables. The most commonly used dimensionless numbers for heat transfer in agitated vessels are:

Reynolds Number: is the ratio between inertial forces to viscous forces, is commonly used to determine the flow regime and for agitated vessels it is defined as follows:

$$Re = \frac{N\,d^2}{\nu} \tag{17}$$

where N is the rotational speed of the impeller in rev/sec, d is the impeller diameter in meters and ν is the kinematic viscosity of the fluid. For agitated vessels, the flow can be considered laminar for Re < 50, transitional for 50 < Re < 5000 and fully turbulent for Re > 5000.

Prandtl Number: is the ratio between kinematic viscosity to thermal diffusivity. Prandtl number doesn't depend upon a characteristic length but only upon the fluid. Therefore it can be found in tables alongside other properties of the fluid and sometimes it can be considered as a constant. It is defined as:

$$Pr = \frac{\nu}{a} = \frac{\mu\,Cp}{\lambda} \tag{18}$$

where μ is the dynamic viscosity, Cp is the specific heat capacity and λ is the thermal conductivity, all of them are properties of the fluid.

Nusselt number: is the ratio between convective and conductive heat transfer. It is defined as:

$$Nu = \frac{\alpha\,D}{\lambda} \tag{19}$$

where α is the heat transfer coefficient of the process, D is the characteristic length (diameter of the vessel) and λ is the thermal conductivity of the fluid. The heat transfer

coefficient describes the heat transfer rate between the fluid and the vessel, therefore is one of the most important parameters within the process.

Swirl number: is the relation between tangential and axial velocity components, it is defined as [Mahmood, 1980]:

$$S = \frac{2\,G_w}{d\,G_u}, \qquad G_w = \int_A \rho\, r\, w\, u\, dA, \qquad G_u = \int_A \rho\, u^2\, dA \qquad (20)$$

where Gw and Gu represent axial fluxes of tangential and axial momentums, respectively. A refers here to the outlet cross-section area of the draft tube.

In the case of forced convection, a general correlation for the Nusselt number could be described as follows:

$$Nu = f(Re, Pr, geometrical\ parameters) \qquad (21)$$

The most common representation for the previous correlation is known as the Dittus-Boelter's correlation, Eq. (22). This is generally used in the case of flow in a pipe, but it can also be useful as a reference for agitated vessels.

$$Nu = 0.023\, Re^{0.8}\, Pr^{\frac{1}{3}} \qquad (22)$$

Petera et al., measured the heat transfer at the bottom of a cylindrical vessel impinged by a swirling flow from an impeller in a draft tube using the electrodiffusion experimental method. They presented the following correlation for the local values of the Nusselt number along the radial coordinate of the heat transfer surface:

$$Nu = 0.041\, Re^{0.826}\, Pr^{\frac{1}{3}}\, S^{0.609} \qquad (23)$$

MODEL DESCRIPTION AND METHODOLOGY

PARAMETERS OF THE MODEL

Simulations for several rotational speeds were performed in ANSYS Fluent, using the SST k-ω turbulent model with the Kato-Launder correction activated [Kato and Launder, 1993]. The geometry was an agitated vessel with 6-blade impeller (pitched blades by 45°) placed in a draft tube and the fluid was water at temperature 300 K, the bottom and wall were heated by a constant heat flux of 30000 W/m^2. Figure 4 shows the geometrical configuration of the model with its dimensions.

H = 430 mm

D = 392 mm

h = 70 mm

d = 70 mm

dm = 61 mm
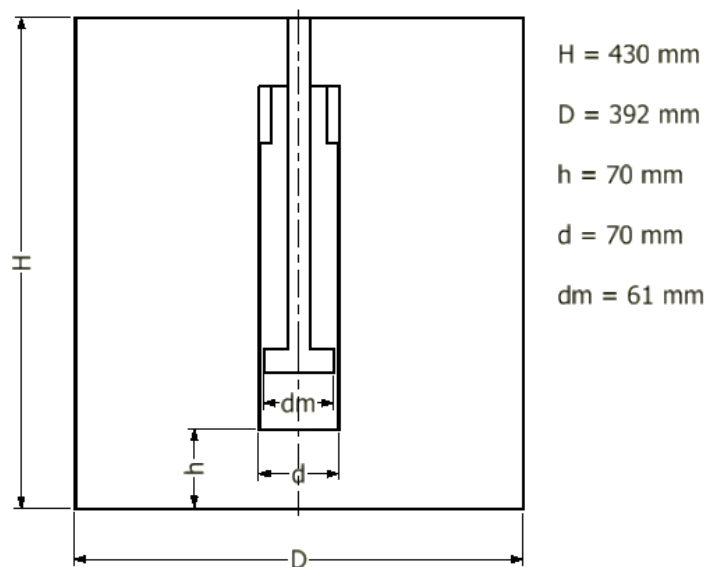
Figure 4 – Geometrical configuration of the model.

The number of mesh elements was more than 3 million, for this reason, the simulations were carried out on the university server with Fluent solver running in the background. An example the scripts used for the simulation is in appendix A (for 300 RPM).

The aforementioned script is divided into three parts, first some steady state iterations were performed with the energy equation switched off. After this, the simulations switches to transient model using the Sliding Mesh approach (which is supposed to be more accurate than MRF). In this part, a time period of 4 seconds is simulated without the energy equation, just to get an initial transient velocity field, and finally 20 seconds are simulated with the energy equation activated and the constant heat flux of 30000 W/m^2.

MESH QUALITY

The mesh created in ANSYS Mesh was modified in ANSYS Fluent to improve the quality by changing the tetrahedral mesh elements into polyhedral. The number of elements was reduced from 3 to 2 million approx. and the orthogonal quality (which ranges from 0 to 1, where values close to 0 correspond to low quality) increased from 0.072 to 0.28. Figure 5 shows the statistics before and after the improvement.

Statistics	
☐ Nodes	2338465
P Elements	3334459
Mesh Metric	Orthogonal Quality ▼
☐ Min	7.1693e-002
☐ Max	1.
☐ Average	0.9251
☐ Standard Deviation	0.10839

```
Mesh Size

Level    Cells    Faces    Nodes    Partitions
    0  2186786  7881035  3669663            16

 2 cell zones, 23 face zones.

Mesh Quality:

Minimum Orthogonal Quality =  2.85585e-01
```
Figure 5 – Top: statistics of the mesh with ANSYS Mesh. Bottom: statistics of the mesh after the improvement in ANSYS Fluent.

The height of the first layer of the mesh at the bottom of the tank (inflation layer) defined in ANSYS Mesh was 0.4 mm.

Y^+ VALUES

As it was mentioned in previous chapters, when we are interested in the heat transfer, the whole viscous sublayer must be described properly and no wall functions are used in such cases. In order to accomplish this, the Y^+ value should be close to 1. After performing the simulations, it was verified that the values of Y^+ satisfied this condition. Figure 6 shows the Y^+ values at the bottom and wall for a rotational speed of 900 RPM.
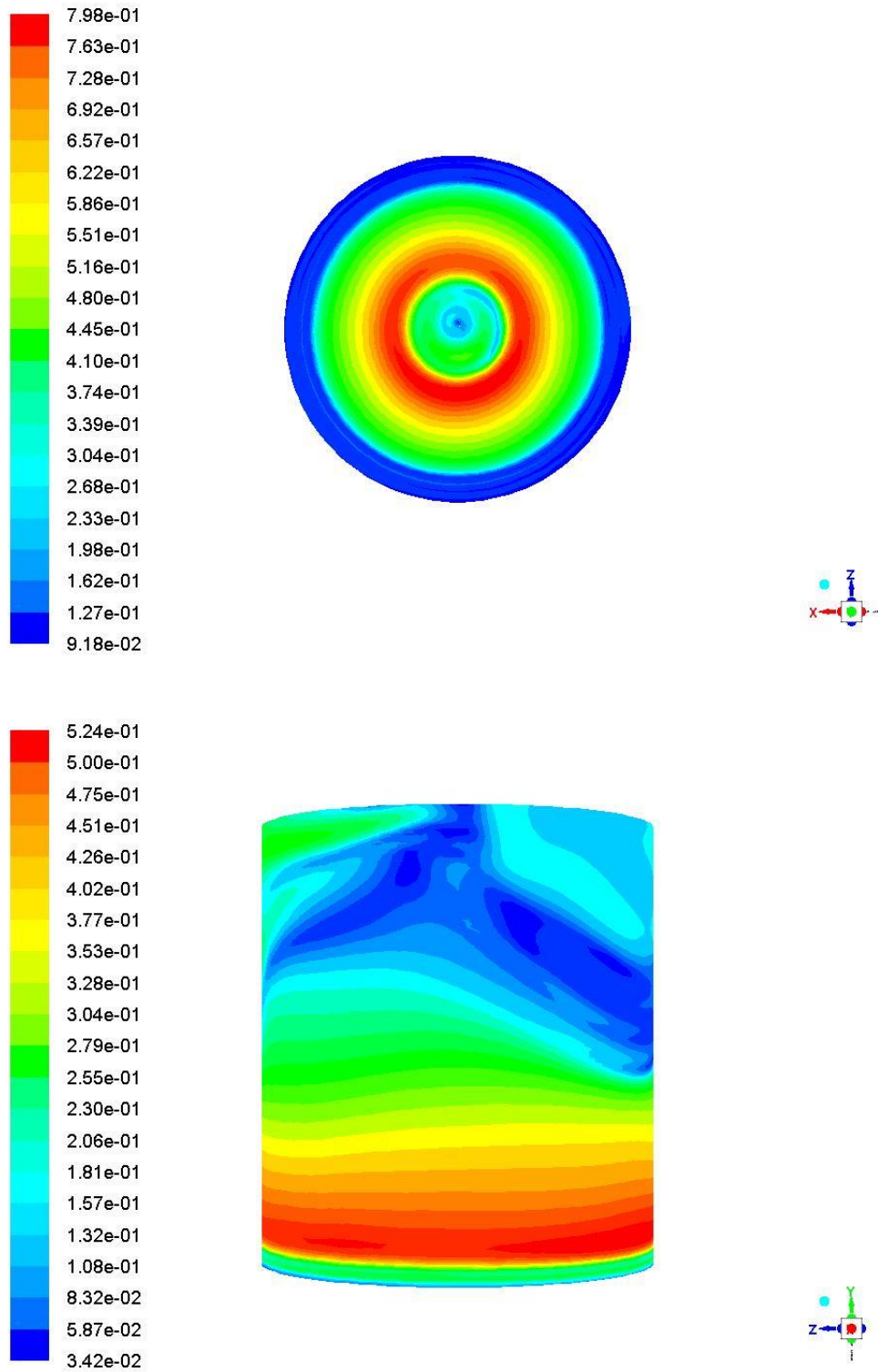
Figure 6 – Top: Values of Y-plus at the bottom of the tank. Bottom: Values of Y-plus at the wall of the tank.

GRID INDEPENCE STUDY

A study based on the number of mesh elements was already done for an agitated vessel by [Chakravarty, 2017]. Therefore, a grid independence study focused on the number of time steps was performed instead. The aim of this study was to select an appropriate time step taking into account the time it takes to perform the simulation. The results of three simulations with a rotational speed of 900 RPM were evaluated. The results are shown in the Table 1.

Size of time step [sec]	0.001	0.05	0.01
Number of time steps	20000	4000	2000
Total wall-clock time [days]	10.4	6.3	5.4
Real time [days]	15-17	8-10	4-6
Total HTC [w/m2-k]	942.13	859.36	1066.41
Total HTC extrapolated [w/m2-k]	1345.8		
GCI	53.56	70.76	32.75

Table 1 – Data of the simulation at 500 RPM with different time steps.

The Grid Convergence Index (GCI) was calculated using Matlab (the script is shown in Appendix B). The monitored quantity was the total Heat Transfer Coefficient (HTC) and the number of time steps was calculated only for the last 20 seconds (when the energy equation is activated). Figure 7 shows the dependence of the Heat Transfer Coefficient on the number of time steps.
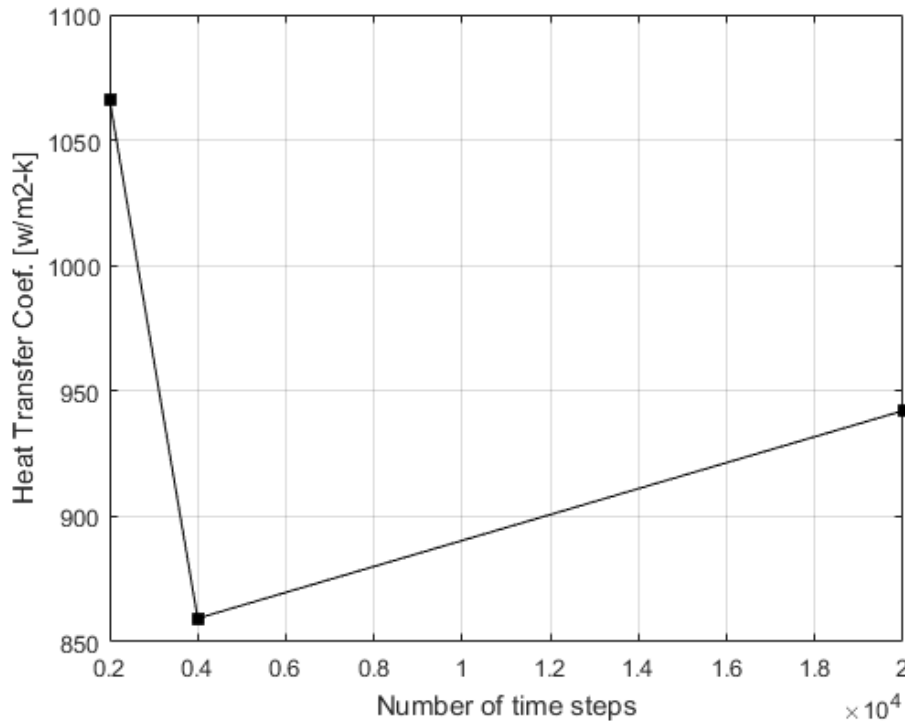
Figure 7 – Dependence of the HTC on the number of time steps for 500 RPM.

The results of the GCI show a non-monotonic dependency of the monitored quantity on the number of time steps (oscillatory tendency with non-decreasing amplitude), where the GCI for the biggest number of time steps (20000) is smaller than the GCI for the middle point (4000) but bigger than the GCI for the smallest number of time steps (2000). The reason for this could be the size of the time step, for Sliding Mesh approach much smaller size of time step should be used. Unfortunately due to this results, is difficult to evaluate the GCI with respect to the number of time steps properly. The main parameter used to choose the size of the time step, was the time that takes to complete the simulation. The simulation with the time step 0.01 seconds took approximately 3 to 5 days at the faculty computational servers and decreasing the size of the time step to 0.005 seconds for the same simulation, the time will increase to 8 to 10 days. Because of the fact that several simulations have to be performed in order to analyze the results, the time step of 0.01 seconds was chosen.

CORRELATIONS FOR THE NUSSELT NUMBER

After defining the size of the time step, simulations for 8 different rotational speed ranging from 200 RPM to 900 RPM were performed. The evaluated quantity was the mean Nusselt number. The bottom of the tank and the wall are heated simultaneously and this results in 3 different Nusselt numbers: at the bottom, at the wall and the total (average of the previous two). Table 2 shows the mean Nusselt numbers obtained from the simulations together with the Reynolds number, which was calculated with Eq. (17) using the dynamic viscosity ($\mu = 0.001003$ Pa s) and density ($\rho = 99.8.2$ kg/m^3) of water.

Rotational speed [RPM]	Nusselt number			Re
	Bottom	Wall	Total	
200	82.59	75.11	76.49	12344
300	108.39	75.83	81.85	18516
400	153.32	80.54	93.99	24688
500	236.31	99.04	124.41	30860
600	263.89	117.97	144.93	37032
700	311.93	142.11	173.49	43204
800	350.51	167.92	201.66	49376
900	387.26	191.27	227.48	55548

Table 2 – Values of the Nusselt and Reynolds number according to the rotational speed.

With the data obtained from the simulation, the aim was to present a correlation for the Nusselt number as follows:

$$Nu = c\, Re^m\, Pr^{1/3} \qquad\qquad (24)$$

Using Matlab functions nlinfit and nlparci a nonlinear regression was perfomed to calculate the coefficients c and m for the previous correlation. Part of the Matlab script is shown below, the full script is shown in Appendix C.

```
fmodel = @(c,R) c(1)*R.^c(2);

[c1,r,J] = nlinfit(Re,B,fmodel,[1 1]);
ci1 = nlparci(c1,r,'Jacobian',J);

NuPrbottom = c1(1)*Re.^c1(2);
```

Table 3 shows the value of the coefficients c and m and their confidence intervals (regions where the best-fit values of the parameter lie with 95% probability) for the Nusselt number at the bottom, at the wall and the total.

	c	Conf. Interval for c	m	Conf. Interval for m
Bottom	0.002	-0.001 - 0.005	1.059	0.903 - 1.215
Wall	0.010	-0.019 - 0.039	0.837	0.561 - 1.114
Total	0.005	-0.005 - 0.016	0.913	0.723 - 1.104

Table 3 – Values of the coefficients for the correlation of Nusselt number.

The correlations can be summarized as follows:

$$Nu_{bottom} = 0.002 \, Re^{1.059} \, Pr^{\frac{1}{3}} \tag{25}$$

$$Nu_{wall} = 0.010 \, Re^{0.837} \, Pr^{\frac{1}{3}} \tag{26}$$

$$Nu_{total} = 0.005 \, Re^{0.913} \, Pr^{\frac{1}{3}} \tag{27}$$

Figure 8 shows the relation between the Nusselt number and the Reynolds number for the correlations obtained with the nonlinear regression and the Dittus-Boelter's correlation, Eq. (22), as well as the data obtained from the simulation, at the bottom, at the wall and the total.

27
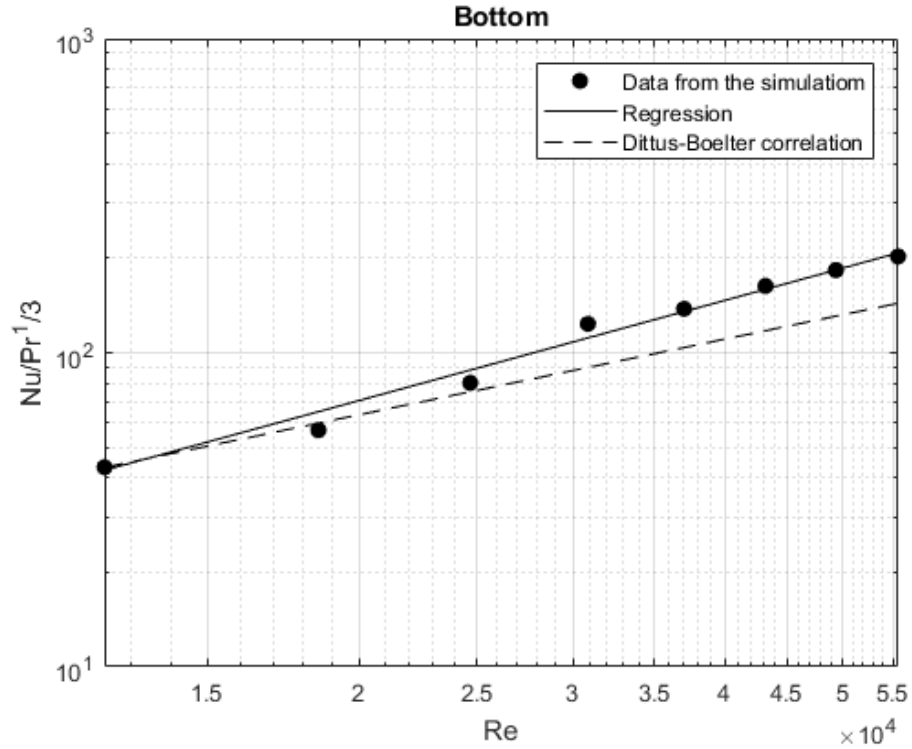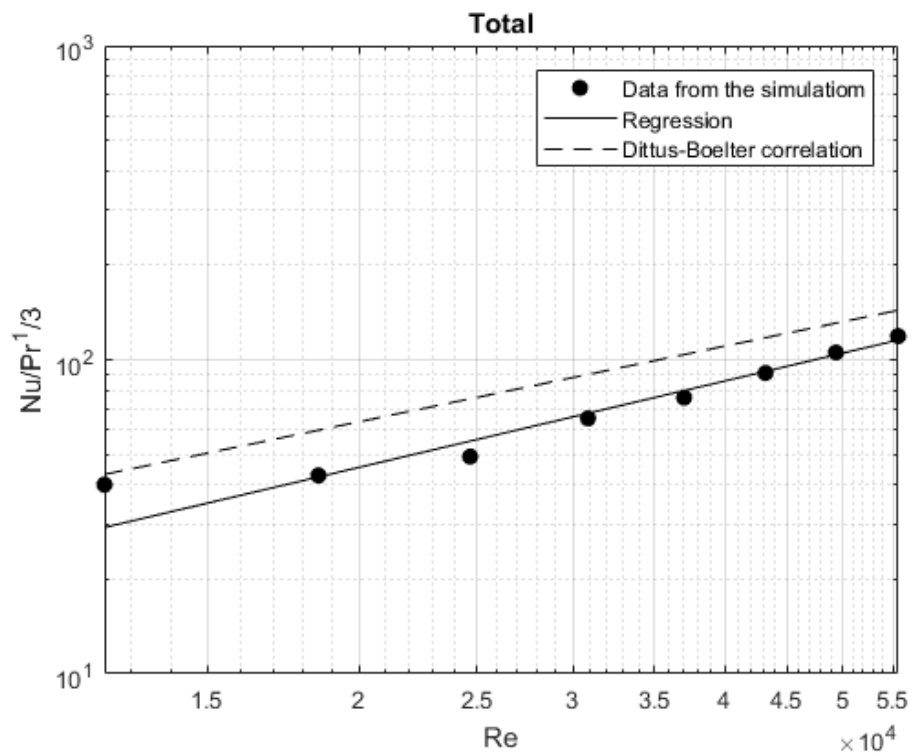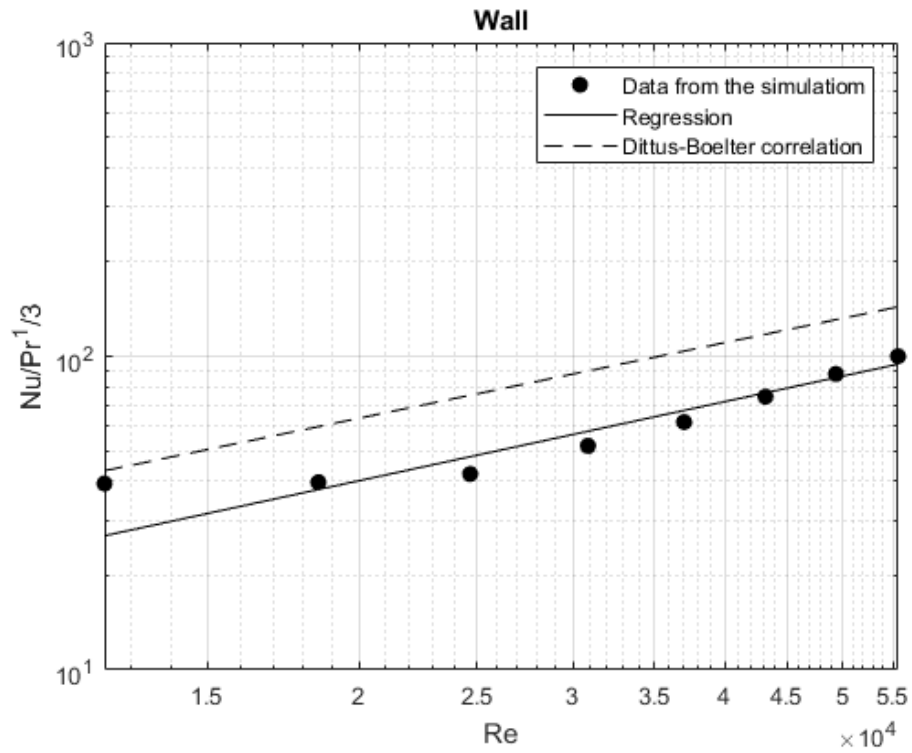
Figure 8 – Correlations obtained from the nonlinear regression and data from the simulation are compared with the literature correlation of Dittus-Boelter.

We can observe from the data in Table 3 that the exponents of the Reynolds number in the correlations are too big, especially for the bottom, which has a value of 1.059 and a confidence interval between 0.903 and 1.215, this means an error of about 15%. In the correlation for the wall, the exponent of the Reynolds number obtained with the regression, is similar to the exponent in the Dittus-Boelter correlation, but the confidence interval is also large, with an error of about 30%. For this reason, another nonlinear regression was performed to compare the results obtained from the simulation with the same correlation of Dittus-Boelter, but this time only the constant c was calculated and the exponent of the Reynolds number used was 0.8. Part of the Matlab script used for the simulation is shown below, the full script is in Appendix D.

```
fmodel = @(c,R) c*R.^0.8;

[c1,r,J] = nlinfit(Re,B,fmodel,1);
ci1 = nlparci(c1,r,'Jacobian',J);   %confidence interval

NuPrbottom = c1*Re.^0.8;
```

Table 4 shows the value of the coefficient c and its confidence interval for the Nusselt number at the bottom, wall and the total.

	c	Conf. Interval - c
Bottom	0.03	0.028 - 0.033
Wall	0.014	0.013 - 0.016
Total	0.017	0.016 - 0.019

Table 4 – Values of the coefficient for the second correlation of Nusselt number (the exponent of the Reynolds number used was 0.8).

The correlations can be summarized as follows:

$$Nu_{bottom} = 0.03 \, Re^{0.8} \, Pr^{\frac{1}{3}} \tag{28}$$

$$Nu_{wall} = 0.014 \, Re^{0.8} \, Pr^{\frac{1}{3}} \tag{29}$$

$$Nu_{total} = 0.017 \, Re^{0.8} \, Pr^{\frac{1}{3}} \tag{30}$$

The new correlations have a stronger impact at the bottom, where the coefficient of 0.03 is very close to the coefficient in the Dittus-Boelter correlation (0.023) and the error decrease

from 15% to 10%. As for the wall, even though the coefficient did not change abruptly (from 0.01 to 0.014), the confidence interval decrease significantly, decreasing the error from 30% to around 10%. Figure 9 shows the relation between the Nusselt number and the Reynolds number for the new correlations at the bottom, wall and total compared with the Dittus-Bolter correlation.
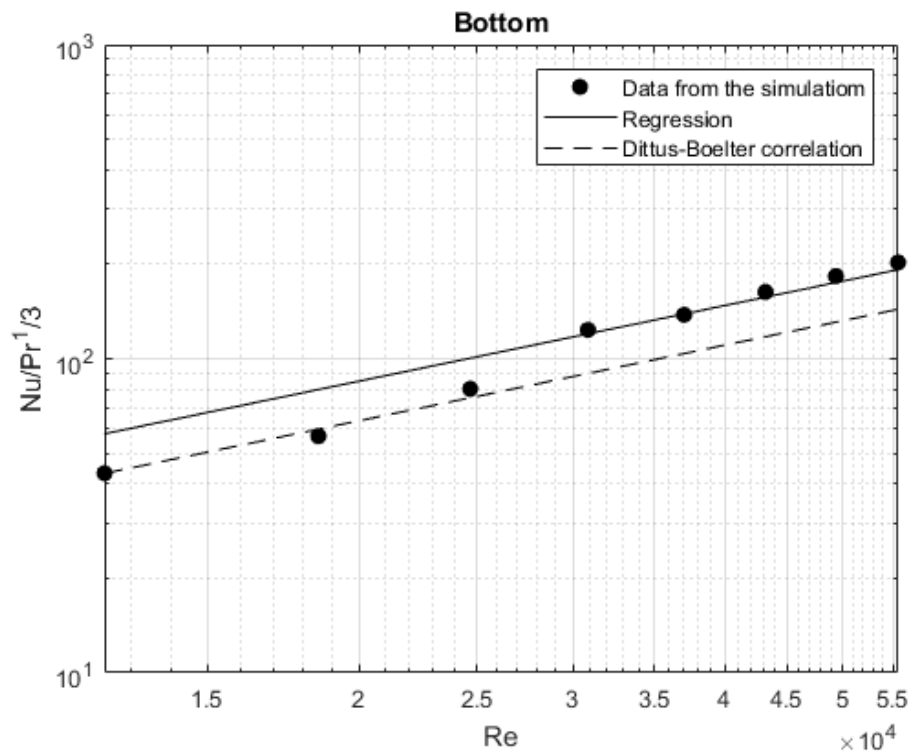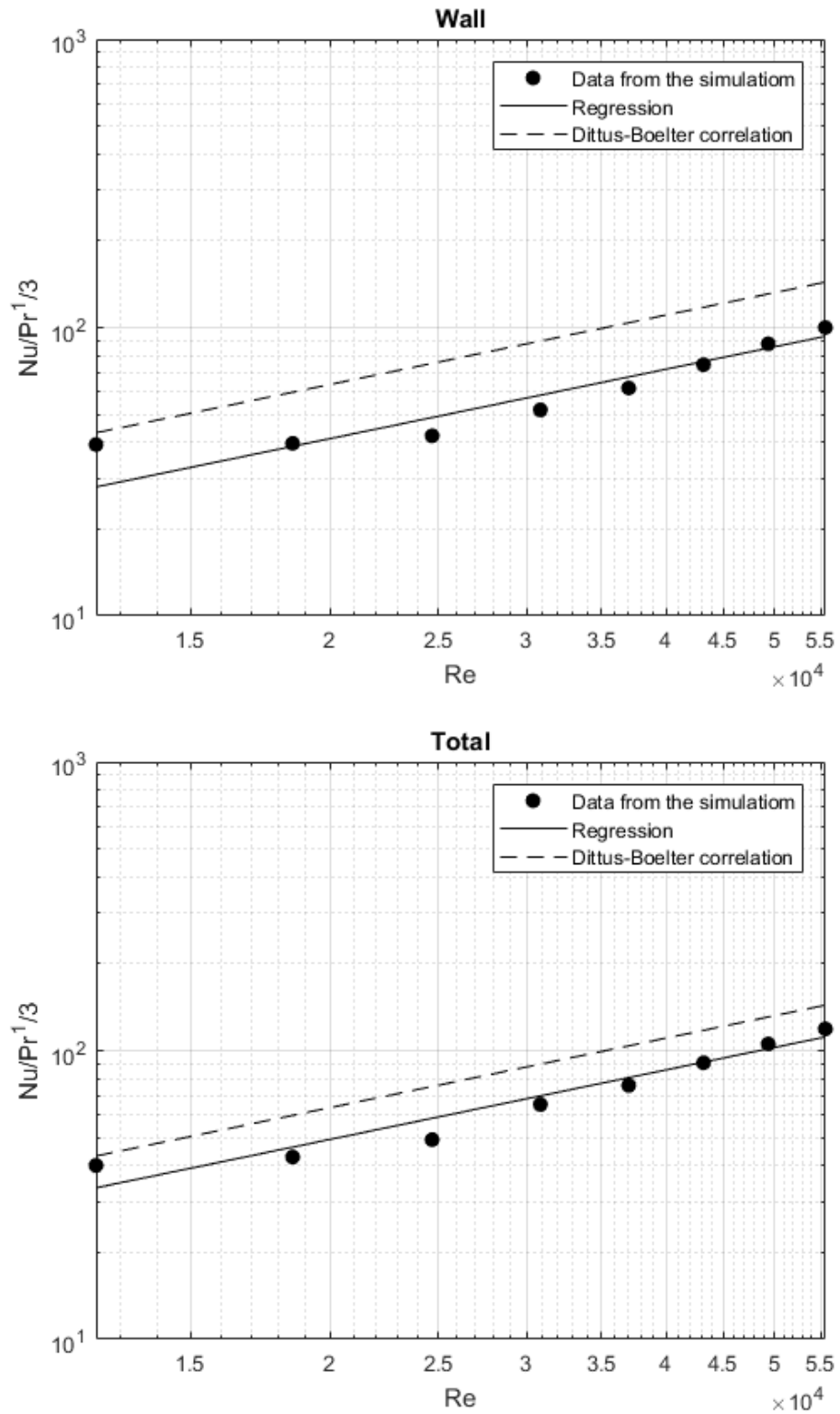
Figure 9 – Correlations obtained from the second nonlinear regression (only the parameter c was calculated and the exponent of the Reynolds number used was 0.8) and data from the simulation are compared with the literature correlation of Dittus-Boelter.

A third nonlinear regression was performed, this time to take into account the effect of the Swirl number, Eq. (20), but the confidence intervals obtained were too big, therefore, no further analysis was possible.

LOCAL VALUES

The local values of the Nusselt number at the bottom were measured for different Reynolds number along the dimensionless radial coordinate r/d, where r is the radio of the tank and d is the diameter of the draft tube. Figure 10 shows the results.
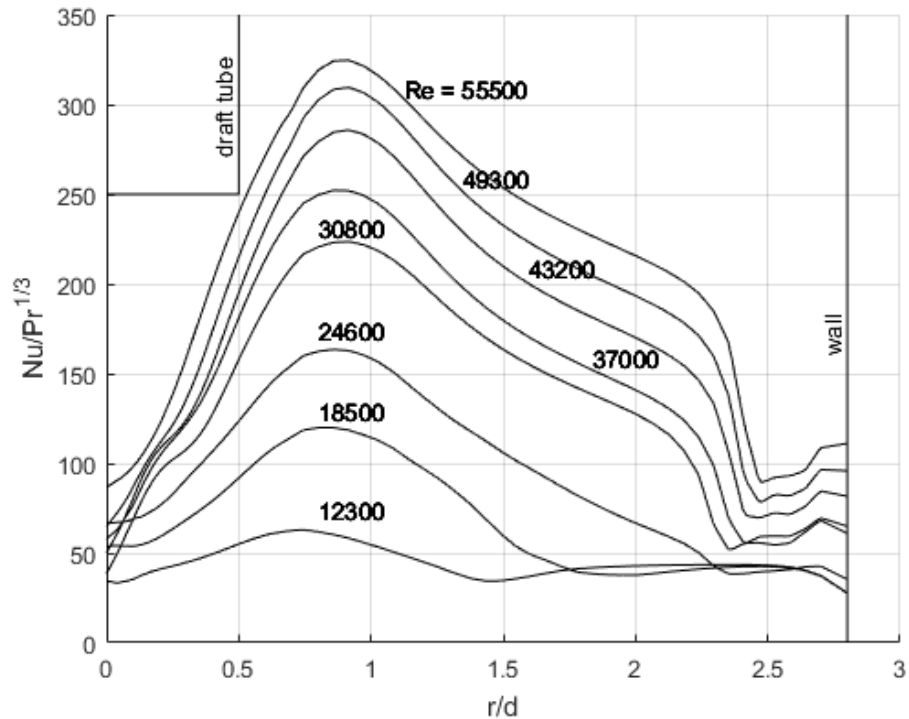
Figure 10 – Local values of the Nusselt number at the bottom for different Reynolds number along the dimensionless coordinate r/d.

We can observe that the highest value of the Nusselt number (and therefore the heat transfer coefficient) is not in the center of the tank, but approximately in the radial dimensionless coordinate r/d = 1. This is due to the tangential velocity, which is also the main difference with the non-swirling impinging jets, where the highest heat transfer coefficient is located closer to the center of the tank (r/d = 0).

32

However, Petera et al. published an experimental study about the heat transfer at the bottom of an agitated vessel, for different dimensionless distances h/d. They state that the effect of the tangential velocity has more impact for smaller distances from the bottom of the vessel and it is very small for dimensionless distance h/d = 1, which is the case of the present project [K. Petera et al, Heat Transfer at the Bottom of a Cylindrical Vessel, 2017].

Concerning the wall, the local values of the Nusselt number were measured for different speed rotations along the dimensionless coordinate y/H, where y is the distance from the bottom and H is the height of the tank. A significant increment was observed from 400 RPM (Re = 25000), with lower rotational speeds, the local values can be considered constants. The highest value is located at the corner (y/H close to 0), this is caused because of the presence of a swirl, which increases the convective heat transfer. This behavior is similar to the local values of Nusselt number along a flat plate, where theoretically the heat transfer coefficient is infinitely large at the beginning. In our case, we do not have an infinitely large value of the Nusselt number, but the peak is located at the beginning. Figure 11 shows the dependence of the local values of Nusselt number for different speed rotations.
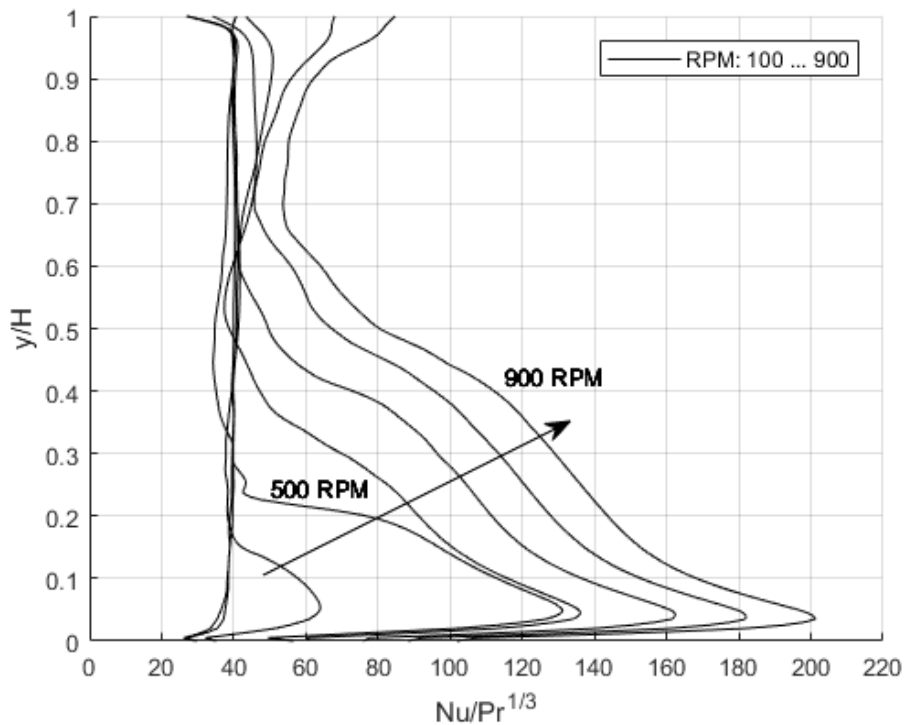
Figure 11 – Local values of the Nusselt number at the wall along the dimensionless coordinate y/H.

INFLUENCE OF SIMULTANEOUS HEATING THE BOTTOM AND WALL

Another simulation at 500 RPM and time step 0.01 was performed, but in this simulation only the bottom was heated. This was done in order to compare the effects of the boundary conditions. In this project, the bottom and the wall are heated simultaneously, but usually the experimental results are based on heating the bottom and the wall separately. The average heat transfer coefficient when only the bottom is heated was 2136.80 [w/m^{2}K] and when bottom and wall are heated simultaneously it was 2025.59 [w/m^{2}K]. If we compare the two values, the difference is approximately 5%. The results of the local values of the Nusselt number along the dimensionless coordinate r/d are depicted in Figure 12.

The main difference is clearly visible in the corner where bottom and wall are connected. The Nusselt number is bigger in the corner when only the bottom is heated because the temperature difference between bottom and wall is bigger (higher heat transfer coefficient).
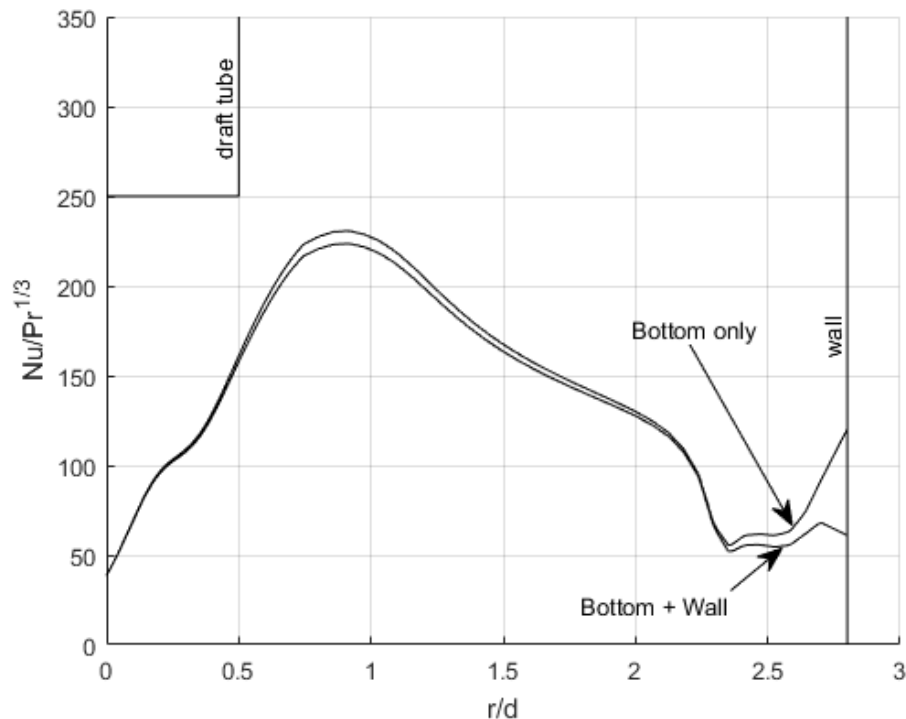

Figure 12 – Local values of the Nusselt number at the bottom along the dimensionless coordinate r/d for two different simulations: only the bottom is heated and the bottom and wall are heated simultaneously (500 RPM, Re = 30000).

COMPARISON WITH PREVIOUS RESULTS

The mean values of the Nusselt number at the bottom obtained with the simulations where compared with existing data from a simulation based on MRF (Moving Reference Frame) approach and heat flux in the bottom only [Petera K., Habilitation thesis, CTU Prague, 2017]. The time step used in the MRF simulation was the same as the one used in our simulations (0.01 sec). The correlation obtained from this simulation was:

$$Nu = 0.101 \, Re^{0.68} \, Pr^{\frac{1}{3}} \tag{31}$$

The confidence interval for the exponent of the Reynolds number was 0.680 ± 0.051 and for the leading constant 0.101 ± 0.055. If we compare this data with Eq. (25) we can see that both, the leading constant and the Reynolds power of the correlation obtained with the MRF approach are different and do not lie within the confidence intervals of the values obtained with the Sliding Mesh approach. One of the reason of these discrepancies (specially the power of the Reynolds number) could be the different boundary conditions, the simulations with the Sliding Mesh approach were performed with a heat flux at the bottom and wall simultaneously, while the simulations with MRF approach were performed with heat flux at the bottom only. Another, and probably the main reason, is the size of the time step. The sliding mesh approach is more sensitive to the size of the time step, which must be sufficiently small. Due to the high computational requirements, and limited capacity of the faculty computational server, it was not possible to perform the simulations with a substantially smaller value of the time step.

Figure 13 shows value of the mean Nusselt number for several Reynolds numbers obtained with MRF and Sliding Mesh approaches and the correlation of Eq. (25) obtained with the nonlinear regression.
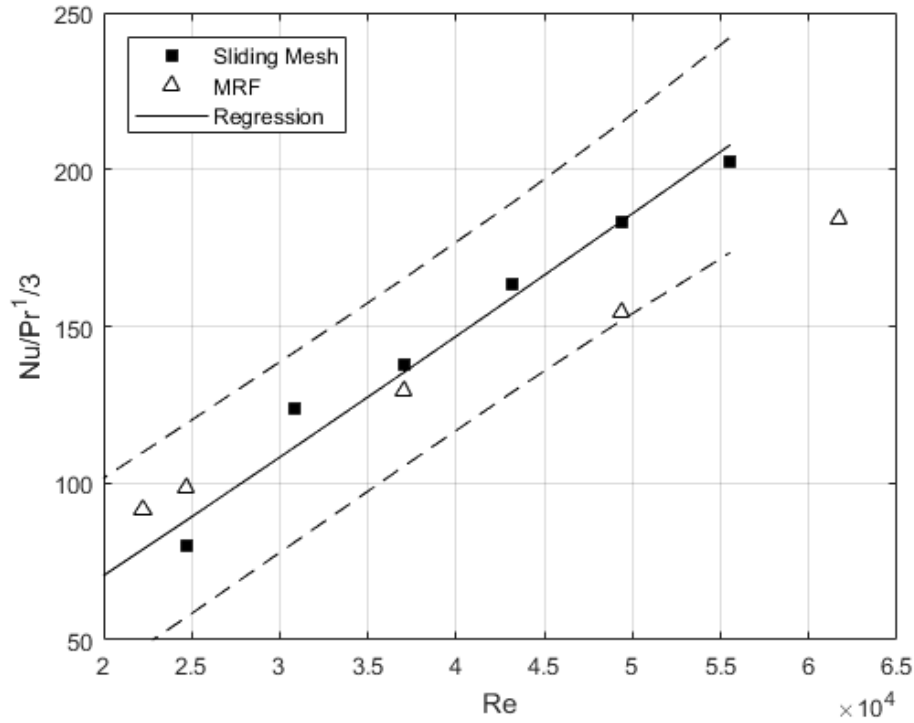
Figure 13 – Values of the mean Nusselt number for several Reynolds number obtained with MRF and Sliding Mesh approaches.

The dashed lines represent the prediction bands of the correlation of Eq. (25), this is the region where 95% of the data would fall if we continue and measure much more data points.

Most of the data obtained with the MRF approach is within the prediction bands, which from the statistical point of view means that the compared data are similar.

VERIFICATION OF FINAL TEMPERATURE

The final temperature can be calculated analytically and compared with the results from the simulation. This will let us know if the simulation has an appropriate behavior and if the results are trustworthy from the physical point of view.

We can start with the main equation to calculate the heat flux:

$$Q = m\,Cp\,\frac{dT}{dt} \tag{32}$$

where m is the total mass of the heated fluid, this can be calculate as the volume of the tank times the density of the water (998 kg/m³.) The specific heat capacity (Cp) is constant and for the water has a value of 4182 [J/kg K]. A heat flux of 30000 W/m² was used (q), so we need to take into account the surface where the heat flux where applied (S), therefore the previous equation can be expressed as:

$$q\,S = V_{tank}\,\rho_{water}\,Cp_{water}\,\frac{dT}{dt} \tag{33}$$

This is an ordinary differential equation, which can be solved by separating the variables and integrating. The limits for the integration in the temperature side are the initial temperature, which is known (300 K) and the final temperature Tf, and for the time side the mixing time, from 0 to 20 seconds. The heat flux, surface, volume of the tank, density of water and specific heat capacity of water are constant.

$$q\,S \int_{0}^{20} dt = V_{tank}\,\rho_{water}\,Cp_{water} \int_{300}^{Tf} dT$$

$$q\,S\,(20 - 0) = V_{tank}\,\rho_{water}\,Cp_{water}\,(Tf - 300)$$

$$Tf = \frac{q\,S\,(20)}{V_{tank}\,\rho_{water}\,Cp_{water}} + 300\,K \tag{34}$$

The heat flux is applied to the bottom and wall, therefore the surface (S), can be calculated as the sum of the bottom surface (πr^2) and the wall surface ($2\pi r \times H$). The diameter of the tank is 392 mm and the height of the tank 430 mm. The total surface (S) is 0.65 m² and the volume of the tank ($\pi r^2 \times H$) is 0.05 m³. By replacing these values in Eq. (34), the final temperature Tf is 301.86 K. The final temperature obtained from the simulation with a report of volume integrals is 301.82 K, which tells us that the calculation is correct.

COMPARISON WITH A LONGER MIXING TIME

Two more simulations were performed at 500 RPM with the same boundary conditions (bottom and wall heated simultaneously) and time step 0.01 sec. but with a longer mixing time, for 30 and 40 seconds. The aim of this was to compare the accuracy of the current results (mixing time of 20 sec.) with the results of a simulation with a longer mixing time.

In order to do this, a similar approach to the grid convergence study was done in Matlab (the Appendix E shows the full script) and the grid convergence indexes were calculated for the Nusselt number at the bottom, wall and total. A decreasing tendency was identified in all the values and the GCI for the results with 20 seconds of mixing time were 8% for the Nusselt number at the bottom, 12% at the wall and 21.07% the total. Table 5 shows the result of the Nusselt number according to the mixing time as well as all the values of the GCI and the extrapolated values of the Nusselt number at the bottom, wall and total.

BOTTOM (Nu-ext = 221.09)		
Mixing time	Nusselt	GCI
20	236.31	8%
30	232.36	6%
40	225.9	2.60%
WALL (Nu-ext = 89.52)		
Mixing time	Nusselt	GCI
20	99.04	12%
30	96.06	8.50%
40	93.84	5.74%
TOTAL (Nu-ext = 103.43)		
Mixing time	Nusselt	GCI
20	124.41	21.07%
30	121.25	18.36%
40	118.25	15.65%

Table 5 – Values of the Nusselt number according to the mixing time, extrapolated values of the Nusselt number and GCI's at the bottom, wall and the total.

For a considerable large mixing time, a correction to eliminate the temperature increase of the fluid in the vessel have to be applied. For the calculation of the heat transfer coefficient, Fluent solver does not take into account this increase but instead, takes the temperature of the fluid as constant input parameter (T_{ref}) according to the following equation:

$$\alpha = \frac{q}{T_{ref} - T_w} \tag{35}$$

where q is the heat flux and T_w is the temperature at the wall.

In this project no correction was necessary because the temperature increase of the fluid after the mixing was relatively small (1.82 K).

CONCLUSIONS AND RECOMMENDATIONS

SUMMARY OF THE WORK DONE

— Simulations of heat transfer in an agitated vessel with draft tube were performed for several rotational speed ranging from 100 to 900 RM. The mesh was modified in ANSYS Fluent to get a better quality. The turbulence model used was the SST k–ω with the Kato-Launder correction and the Sliding Mesh approach, which is supposed to be more accurate than Moving Reference Frame (MRF) approach.

— A Grid Independence Study focused on the time step was performed to determine the appropriate size of the time step for the simulations. The Grid Convergence Index (GCI) shows an oscillatory tendency with non-decreasing amplitude. Therefore, it was not possible to evaluate a reasonable value of the GCI. Based on the time it takes to complete the simulation (3 to 5 days) the time step of 0.01 seconds was chosen.

— Correlations for the mean Nusselt number at the bottom, wall and total were evaluated. Non-linear regressions in Matlab were performed to determine the coefficients and the results were compared with the Dittus-Boelter correlation.

— The local values of the Nusselt number at the bottom and wall were evaluated. Results at the bottom show a peak where r/d is approximately 1. As for the wall, the highest value is close to the corner, where y/H is close to 0.

— The mean values of the Nusselt number at the bottom were compared with results of previous simulations, which was performed using the Moving Reference Frame approach. In both cases, similar values for the Nusselt number can be found for Reynolds number between 3000 and 4000.

— The influence of the simulation time on the accuracy of the results was evaluated using a similar approach to the grid convergence study. The difference of the accuracy between the actual and extrapolated value for the mixing time of 20 seconds was 8% at the bottom and 12% at the wall.

RECOMMENDATIONS

— With the Sliding Mesh approach, much smaller time step must be used to obtain more accurate results. It was not possible to repeat the simulations with a smaller time step due to high computational requirements and insufficient capacity of the faculty computational servers.

— It could be possible to increase the mixing time in order to get more accurate results, which would, of course, increase the simulation time. A correction eliminating the temperature increase of the liquid in the vessel would have to be applied in case when this cannot be neglected (see Chakravaty, 2017).

— A different turbulent model could be used to perform new simulations and compare the results with the present work.

REFERENCES

1. A. Chakravarty, CFD simulation of Heat Transfer in Agitated Vessel, Master Thesis, Czech Technical University in Prague, Czech Republic (2017).
2. ANSYS Training material (2014).
3. J. Geankoplis, Transport Processes and Separation Process Principles, Prentice Hall (2003).
4. Celik, I., Numerical Uncertainty in Fluid Flow Calculations: Needs for Future Research, ASME JOURNAL OF FLUIDS ENGINEERING, 115, pp. 194-195 (1993).
5. C. Wilcox, Turbulence Modeling for CFD (2006).
6. J. O. Hinze, Turbulence, McGraw-Hill, New York (1975).
7. K. Petera et al., Heat Transfer at the Bottom of a Cylindrical Vessel, Chemical and Biochemical Engineering Quarterly (2017).
8. K. Petera, M. Dostál, F. Rieger, Transient measurement of heat transfer coefficient in agitated vessel, CHISA conference, Czech Republic (2008).
9. K. Petera, Tutorial CFD (2018).
10. K. Petera, Tutorial Momentum Heat and Mass Transfer (2017).
11. M. Kato, B. Launder, The modelling of turbulent flow around stationary and vibrating squares cylinders, 9th Symposium of Turbulent Shear Flows (1993).
12. M. Mahmood, Heat transfer from swirling impinging jets, PhD. Thesis, Cranfield Institute of Technology (1980).
13. R. B. Bird, W.E Stewart, E. N. Lightfoot, Transport Phenomena (2017).

APPENDIX

A) SCRIPT FOR THE SIMULATION OF 300 RPM.

```
; fluent172r 3ddp -t 12 -g -i fluent.in
/file/read-case-data init.cas.gz
; will overwrite files without a confirmation
/file/confirm-overwrite no
/mesh/reorder/reorder-domain
; rotation speed definition
/define/parameters/input-parameters edit "rotation_speed" "rotation_speed" 300
; first - switch energy off and perform some steady-state iterations
;/define/models energy no
/solve/set/equations/temperature no
/define/models steady yes
;/define/models/viscous/turbulence-expert/kato-launder-model yes
/solve/set/reporting-interval 1
;/solve/monitors/residual/convergence-criteria 1e-4 1e-3 1e-3 1e-3 1e-3 1e-3
/solve/monitors/residual/convergence-criteria 1e-3 1e-3 1e-3 1e-3 1e-3 1e-3
;/solve/iterate 2
/solve/iterate 200
; save steady-state
/file/write-case-data steady.cas.gz
/parallel/timer/usage
;(solver-cpu-time)
; switch to transient model
/define/models unsteady-1st-order yes
; switch energy on + dissipation: no, pressure work: no, kinetic energy: no,
;   diffusion at inlets: yes
;/define/models energy yes no no no yes
;/solve/monitors/residual/convergence-criteria 1e-4 1e-3 1e-3 1e-3 1e-7 1e-3 1e-3
; switch to Sliding Mesh
/define/boundary-conditions/modify-zones/mrf-to-sliding-mesh fluid-inner ()
; switch to MRF
;/define/boundary-conditions/modify-zones/copy-mesh-to-mrf-motion fluid-inner ()
/solve/set time-step 0.01
;/solve/set max-iterations-per-time-step 20
/solve/set data-sampling yes 1 yes yes yes
;/solve/set data-sampling yes 1 yes yes yes no
/solve/set extrapolate-vars yes
(rpsetvar 'flow-time 0.0)
; init statistics
/solve/init/init-flow-statistics
;/define/models/energy yes no no no yes
;/define/boundary-conditions/wall vessel_bottom 0 no 0 no yes heat-flux no 30000 no
no no no 0 no 0.5 no 1
```

;/define/boundary-conditions/wall vessel_wall 0 no 0 no yes heat-flux no 30000 no no no no 0 no 0.5 no 1
; start with 4s time period to get an initial transient velocity field, without energy equation
;/solve/set/equations/temperature yes
;/solve/patch 8 9 () temperature 300
/solve/set/reporting-interval 1
;/solve/dti 1 2
/solve/dti 400 20
/parallel/timer/usage
/solve/initialize/init-flow-statistics
;/solve/patch fluid-inner fluid-outer () temperature 300
/solve/patch 8 9 () temperature 300
/solve/set/equations/temperature yes
wcd trans-0s.cas.gz
; and longer time interval, 20 s, with energy transport + statistics over the time interval
;/solve/dti 3 2
/solve/dti 2000 20
/solve/initialize/show-time-sampled
/parallel/timer/usage
;(solver-cpu-time)
/report/reference-values/length 0.07
/report/reference-values/temperature 300
; bottom lines
/file/write-profile "mean-line-1-full.prof" line-bottom-1-full () radial-coordinate temperature mean-temperature heat-flux mean-heat-flux heat-transfer-coef mean-heat-transfer-coef nusselt-number mean-nusselt-number ()
/file/write-profile "mean-line-2-full.prof" line-bottom-2-full () radial-coordinate temperature mean-temperature heat-flux mean-heat-flux heat-transfer-coef mean-heat-transfer-coef nusselt-number mean-nusselt-number ()
/file/write-profile "mean-line-12-full.prof" line-bottom-12-full () radial-coordinate temperature mean-temperature heat-flux mean-heat-flux heat-transfer-coef mean-heat-transfer-coef nusselt-number mean-nusselt-number ()
/file/write-profile "mean-line-21-full.prof" line-bottom-21-full () radial-coordinate temperature mean-temperature heat-flux mean-heat-flux heat-transfer-coef mean-heat-transfer-coef nusselt-number mean-nusselt-number ()
; vertical lines
/file/write-profile "mean-line-wall-1.prof" line-wall-1 () y-coordinate temperature mean-temperature heat-flux mean-heat-flux heat-transfer-coef mean-heat-transfer-coef nusselt-number mean-nusselt-number ()
/file/write-profile "mean-line-wall-2.prof" line-wall-2 () y-coordinate temperature mean-temperature heat-flux mean-heat-flux heat-transfer-coef mean-heat-transfer-coef nusselt-number mean-nusselt-number ()

/file/write-profile "mean-line-wall-3.prof" line-wall-3 () y-coordinate temperature mean-temperature heat-flux mean-heat-flux heat-transfer-coef mean-heat-transfer-coef nusselt-number mean-nusselt-number ()
/file/write-profile "mean-line-wall-4.prof" line-wall-4 () y-coordinate temperature mean-temperature heat-flux mean-heat-flux heat-transfer-coef mean-heat-transfer-coef nusselt-number mean-nusselt-number ()
/file/write-profile "mean-line-wall-5.prof" line-wall-5 () y-coordinate temperature mean-temperature heat-flux mean-heat-flux heat-transfer-coef mean-heat-transfer-coef nusselt-number mean-nusselt-number ()
/file/write-profile "mean-line-wall-6.prof" line-wall-6 () y-coordinate temperature mean-temperature heat-flux mean-heat-flux heat-transfer-coef mean-heat-transfer-coef nusselt-number mean-nusselt-number ()
/file/write-profile "mean-line-wall-7.prof" line-wall-7 () y-coordinate temperature mean-temperature heat-flux mean-heat-flux heat-transfer-coef mean-heat-transfer-coef nusselt-number mean-nusselt-number ()
/file/write-profile "mean-line-wall-8.prof" line-wall-8 () y-coordinate temperature mean-temperature heat-flux mean-heat-flux heat-transfer-coef mean-heat-transfer-coef nusselt-number mean-nusselt-number ()
wcd trans-20s.cas.gz
/define/custom-field-functions/load "swirl2.scm"
;/report/surface-integrals integral 17 () custom-function-gtheta no
;/report/surface-integrals integral 17 () custom-function-gx no
/report/surface-integrals integral 17 () custom-function-mean-gtheta no
/report/surface-integrals integral 17 () custom-function-mean-gx no
;/define/custom-field-functions/delete custom-function-gx custom-function-gtheta ()
;/report/surface-integrals integral 17 () mean-y-velocity no
/report/surface-integrals integral plane-70-difusor-out () mean-y-velocity no
;/report/surface-integrals area-weighted-avg vessel_bottom () mean-heat-transfer-coef no
;/report/surface-integrals area-weighted-avg vessel_wall () mean-heat-transfer-coef no
;/report/surface-integrals area-weighted-avg vessel_bottom () mean-nusselt-number no
;/report/surface-integrals area-weighted-avg vessel_wall () mean-nusselt-number no
/report/surface-integrals area-weighted-avg vessel_bottom vessel_wall () mean-heat-transfer-coef no
/report/surface-integrals area-weighted-avg vessel_bottom vessel_wall () mean-nusselt-number no
/solve/initialize/show-time-sampled
/parallel/timer/usage
;(solver-cpu-time)
/exit
yes

B) MATLAB SCRIPT FOR THE CALCULATION OF THE GCI AT 500 RPM.

```
Phi = [1066.41 859.36 942.13]; % Heat transfer coef.
N = [2000 4000 20000]; % Number of time steps


r21 = N(1)/N(2);
r32 = N(2)/N(3);


eps32 = Phi(3)-Phi(2);
eps21 = Phi(2)-Phi(1);
s = sign(eps32/eps21);


fq = @(p) log((r21.^p-s)./(r32.^p-s));
fp = @(p) p - 1/log(r21)*abs(log(abs(eps32/eps21)))+fq(p);
p = fzero(fp,1)


Phiext = (Phi(1)*r21.^p -Phi(2))/(r21.^p-1)


t = 2000:1:20000;
li = spline(N,Phi,t);
plot(N,Phi,'sk', N,Phi,'k', 'MarkerFaceColor',[0 0 0])
xlabel('Number of time steps')
ylabel('Heat Transfer Coef. [w/m2-k]')
grid on;


CGI1 = 1.25*abs(Phiext-Phi(1))/Phi(1)*100;


CGI2 = 1.25*abs(Phiext-Phi(2))/Phi(2)*100;


CGI3 = 1.25*abs(Phiext-Phi(3))/Phi(3)*100;
```

C) MATLAB SCRIPT FOR THE NONLINEAR REGRESSION

```
rho = 998.2; mu = 0.001003; nu = mu/rho;
lambda = 0.6; cp = 4182;
a = lambda/(rho*cp); % thermal diffusivity
Pr = nu/a;
Pr3 = Pr^(1/3);

d = load('Data1.txt');

Re = d(:,2);    %Reynolds number
B = d(:,3)/Pr3; %Nu/Pr^1/3 at the bottom
W = d(:,4)/Pr3; %Nu/Pr^1/3 at wall
N = d(:,5)/Pr3; %Nu/Pr^1/3 total

NuPr = 0.023*Re.^0.8; %Dittus-Boelter correlation

%Model function
fmodel = @(c,R) c(1)*R.^c(2);

[c1,r,J] = nlinfit(Re,B,fmodel,[1 1]);
ci1 = nlparci(c1,r,'Jacobian',J);  %confidence interval

NuPrbottom = c1(1)*Re.^c1(2);

figure(1)
loglog(Re,B,'ok', Re,NuPrbottom,'k', Re,NuPr,'k--', 'MarkerFaceColor',[0 0 0]);
xlabel('Re')
ylabel('Nu/Pr^1/3')
grid on;
title ('Bottom')
legend('Data from the simulatiom','Regression','Dittus-Boelter correlation');

hold on;

[c2,r,J] = nlinfit(Re,W,fmodel,[1 1]);
ci2 = nlparci(c2,r,'Jacobian',J);  %confidence interval

NuPrwall = c2(1)*Re.^c2(2);

figure(2)
loglog(Re,W,'ok', Re,NuPrwall,'k', Re,NuPr,'k--', 'MarkerFaceColor',[0 0 0]);
xlabel('Re')
ylabel('Nu/Pr^1/3')
```

```
grid on;
title ('Wall')
legend('Data from the simulatiom','Regression','Dittus-Boelter correlation');

hold on;

[c3,r,J] = nlinfit(Re,N,fmodel,[1 1]);
ci3 = nlparci(c3,r,'Jacobian',J);  %confidence interval

NuPrtotal = c3(1)*Re.^c3(2);

figure(3)
loglog(Re,N,'ok', Re,NuPrtotal,'k', Re,NuPr,'k--', 'MarkerFaceColor',[0 0 0]);
xlabel('Re')
ylabel('Nu/Pr^1/3')
grid on;
title ('Total')
legend('Data from the simulatiom','Regression','Dittus-Boelter correlation');
```

D) MATLAB SCRIPT FOR THE NONLINEAR REGRESSION

```
rho = 998.2; mu = 0.001003; nu = mu/rho;
lambda = 0.6; cp = 4182;
a = lambda/(rho*cp); % thermal diffusivity
Pr = nu/a;
Pr3 = Pr^(1/3);

d = load('Data1.txt');

Re = d(:,2);    %Reynolds number
B = d(:,3)/Pr3; %Nu/Pr^1/3 at the bottom
W = d(:,4)/Pr3; %Nu/Pr^1/3 at wall
N = d(:,5)/Pr3; %Nu/Pr^1/3 total

NuPr = 0.023*Re.^0.8; %Dittus-Boelter correlation

%Model function
fmodel = @(c,R) c*R.^0.8;

[c1,r,J] = nlinfit(Re,B,fmodel,1);
ci1 = nlparci(c1,r,'Jacobian',J);  %confidence interval

NuPrbottom = c1*Re.^0.8;

figure(1)
loglog(Re,B,'ok', Re,NuPrbottom,'k', Re,NuPr,'k--', 'MarkerFaceColor',[0 0 0]);
xlabel('Re')
ylabel('Nu/Pr^1/3')
grid on;
title ('Bottom')
legend('Data from the simulatiom','Regression','Dittus-Boelter correlation');

hold on;

[c2,r,J] = nlinfit(Re,W,fmodel,1);
ci2 = nlparci(c2,r,'Jacobian',J);  %confidence interval

NuPrwall = c2*Re.^0.8;

figure(2)
loglog(Re,W,'ok', Re,NuPrwall,'k', Re,NuPr,'k--', 'MarkerFaceColor',[0 0 0]);
xlabel('Re')
ylabel('Nu/Pr^1/3')
```

```
grid on;
title ('Wall')
legend('Data from the simulatiom','Regression','Dittus-Boelter correlation');

hold on;

[c3,r,J] = nlinfit(Re,N,fmodel,1);
ci3 = nlparci(c3,r,'Jacobian',J);  %confidence interval

NuPrtotal = c3*Re.^0.8;

figure(3)
loglog(Re,N,'ok', Re,NuPrtotal,'k', Re,NuPr,'k--', 'MarkerFaceColor',[0 0 0]);
xlabel('Re')
ylabel('Nu/Pr^1/3')
grid on;
title ('Total')
legend('Data from the simulatiom','Regression','Dittus-Boelter correlation');
```

E) MATLAB SCRIPT FOR EVALUATING THE INFLUENCE OF THE SIMULATION TIME

```
PhiBottom = [236.31 232.36 225.9]; % Nusselt number
PhiWall = [99.04 96.06 93.84]
PhiTotal = [124.41 121.25 118.25]
N = [20 30 40]; % Mixing time

r21 = N(1)/N(2);
r32 = N(2)/N(3);
r13 = N(1)/N(3);

eps32Bottom = PhiBottom(3)-PhiBottom(2);
eps21Bottom = PhiBottom(2)-PhiBottom(1);
sBottom = sign(eps32Bottom/eps21Bottom);

eps32Wall = PhiWall(3)-PhiWall(2);
eps21Wall = PhiWall(2)-PhiWall(1);
sWall = sign(eps32Wall/eps21Wall);

eps32Total = PhiTotal(3)-PhiTotal(2);
eps21Total = PhiTotal(2)-PhiTotal(1);
sTotal = sign(eps32Total/eps21Total);

fqBottom = @(pBottom) log((r21.^pBottom-sBottom)./(r32.^pBottom-sBottom));
fpBottom = @(pBottom) pBottom -
1/log(r21)*abs(log(abs(eps32Bottom/eps21Bottom)))+fqBottom(pBottom);
pBottom = fzero(fpBottom,1)

fqWall = @(pWall) log((r21.^pWall-sWall)./(r32.^pWall-sWall));
fpWall = @(pWall) pWall -
1/log(r21)*abs(log(abs(eps32Wall/eps21Wall)))+fqWall(pWall);
pWall = fzero(fpWall,1)

fqTotal = @(pTotal) log((r21.^pTotal-sTotal)./(r32.^pTotal-sTotal));
fpTotal = @(pTotal) pTotal -
1/log(r21)*abs(log(abs(eps32Total/eps21Total)))+fqTotal(pTotal);
pTotal = fzero(fpTotal,1)

PhiextBottom = (PhiBottom(3)*r13.^pBottom -PhiBottom(1))/(r13.^pBottom-1)
PhiextWall = (PhiWall(3)*r13.^pWall -PhiWall(1))/(r13.^pWall-1)
PhiextTotal = (PhiTotal(3)*r13.^pTotal -PhiTotal(1))/(r13.^pTotal-1)
```

```
figure(1)
plot(N,PhiBottom,'sk', N,PhiBottom,'k', 'MarkerFaceColor',[0 0 0])
xlabel('Simulation time [sec]')
ylabel('Nusselt number')
grid on;

figure(2)
plot(N,PhiWall,'sk', N,PhiWall,'k', 'MarkerFaceColor',[0 0 0])
xlabel('Simulation time [sec]')
ylabel('Nusselt number')
grid on;

figure(3)
plot(N,PhiTotal,'sk', N,PhiTotal,'k', 'MarkerFaceColor',[0 0 0])
xlabel('Simulation time [sec]')
ylabel('Nusselt number')
grid on;

CGIBottom1 = 1.25*abs(PhiextBottom-PhiBottom(1))/PhiBottom(1)*100;
CGIBottom2 = 1.25*abs(PhiextBottom-PhiBottom(2))/PhiBottom(2)*100;
CGIBottom3 = 1.25*abs(PhiextBottom-PhiBottom(3))/PhiBottom(3)*100;

CGIWall1 = 1.25*abs(PhiextWall-PhiWall(1))/PhiWall(1)*100;
CGIWall2 = 1.25*abs(PhiextWall-PhiWall(2))/PhiWall(2)*100;
CGIWall3 = 1.25*abs(PhiextWall-PhiWall(3))/PhiWall(3)*100;

CGITotal1 = 1.25*abs(PhiextTotal-PhiTotal(1))/PhiTotal(1)*100;
CGITotal2 = 1.25*abs(PhiextTotal-PhiTotal(2))/PhiTotal(2)*100;
CGITotal3 = 1.25*abs(PhiextTotal-PhiTotal(3))/PhiTotal(3)*100;
```